Supplementary Materials for:

A gut microbial metabolite of dietary polyphenols reverses obesity-driven hepatic steatosis

Authors: Lucas J. Osborn, Karlee Schultz, William Massey, Beckey DeLucia, Ibrahim Choucair, Venkateshwari Varadharajan, Rakhee Banerjee, Kevin Fung, Anthony J. Horak III, Danny Orabi, Ina Nemet, Laura E. Nagy, Zeneng Wang, Daniela S. Allende, Belinda B. Willard, Naseer Sangwan, Adeline M. Hajjar, Christine McDonald, Philip P. Ahern, Stanley L. Hazen, J. Mark Brown, Jan Claesen

Correspondence to: brownm5@ccf.org and claesej@ccf.org

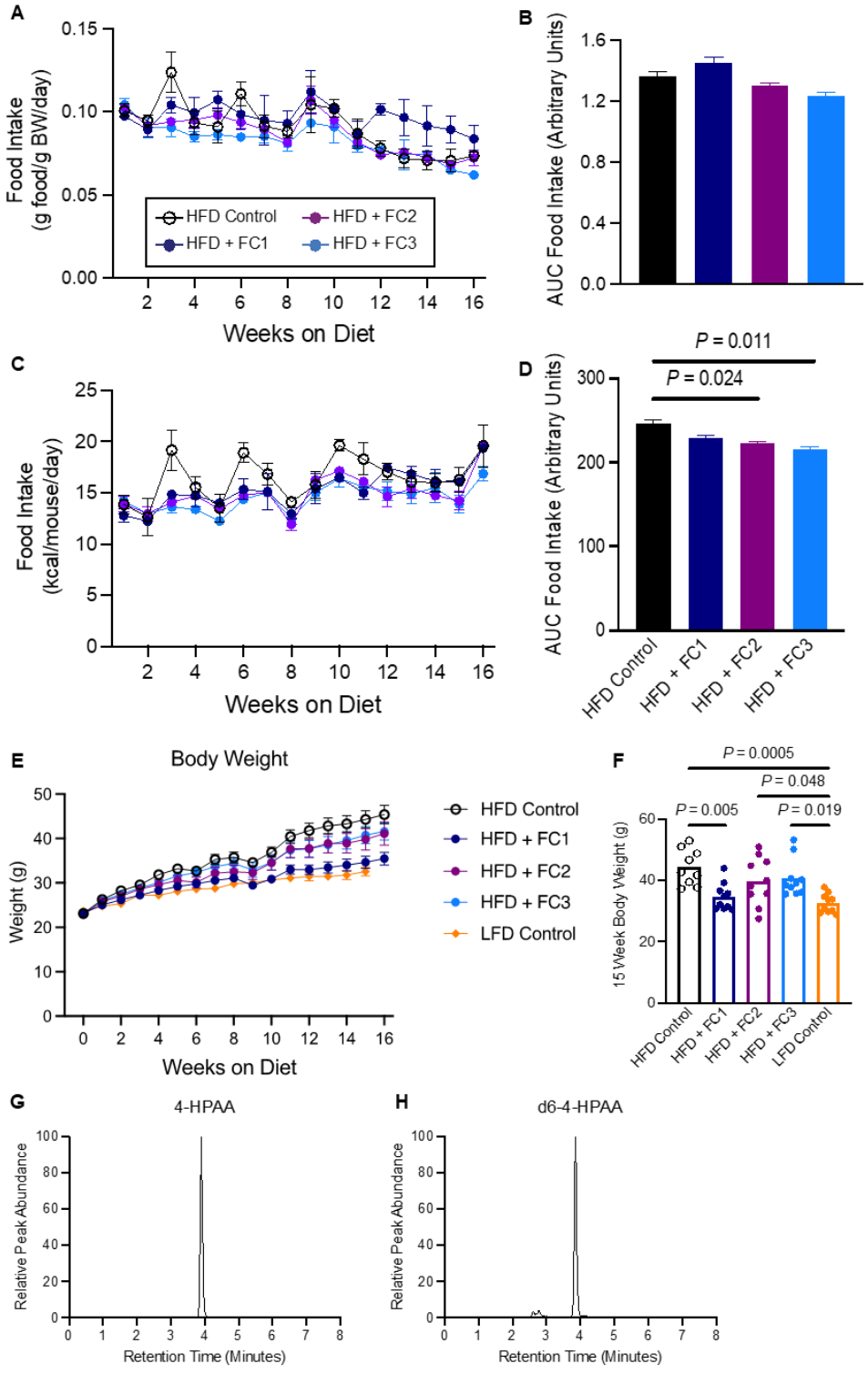

Fig. S1. Flavonoid composites do not impact food consumption but modulate the gut microbial community structure. (**A**) Weekly food consumption data represented

as grams of food consumed per gram of body weight per day. (**B**) Mean cumulative AUC for food intake as represented in panel A; ordinary one-way ANOVA with Dunnett's multiple comparisons test with error bars representing SEM. n=9-10 per group. (**C**) Weekly food consumption data represented as kcal consumed per gram of body weight per day. (**D**) Mean cumulative AUC for food intake as represented in panel C; one-way ANOVA with Tukey's multiple comparisons test with error bars representing SEM. n=9-10 per group. (**E**) Body weights of age and sex matched data from mice eating a low fat diet (LFD) for 15 weeks compared to the experimental groups in Fig. 1A. (**F**) 15-week body weights for LFD, HFD and HFD + FC mice. N=9-10 per group, one-way ANOVA with Tukey's multiple comparisons test. Only *P* values <0.05 are shown. (**G**) and (**H**) Chromatograms representing the relative peak abundance of 4-HPAA and d6-4-HPAA at 50 μM as measured by LC-MS/MS. Individual points represent individual mice, and bars represent group means.

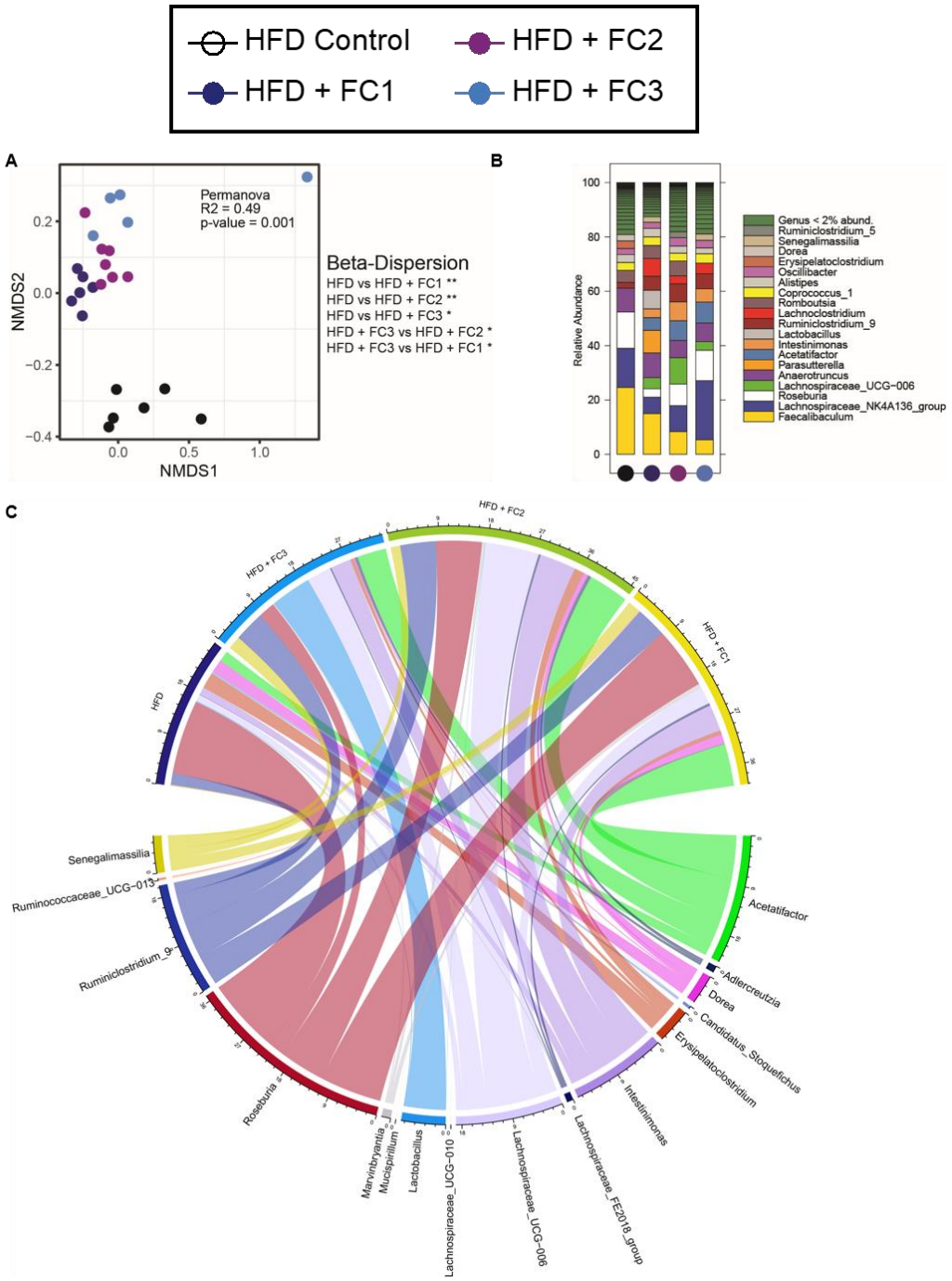

Fig. S2. Feeding different flavonoid composites shifts the cecal microbiota composition in a distinguishable manner. (**A**) NMDS plots based on the Bray-Curtis index between the cecal 16S rRNA profile of all four groups. Statistical analysis was performed with PERMANOVA where R2 values are noted for comparisons with

significant p-values and stand for percentage variance explained by the variable of interest. (**B**) Stacked bar chart of relative abundance (left y-axis) of the top 20 genera assembled across the cecal 16S rRNA profiles of all four groups. N=6 for all 16S rRNA sequence analysis. (**C**) Circle plot comparing the significantly differentially abundant genera between the dietary groups.

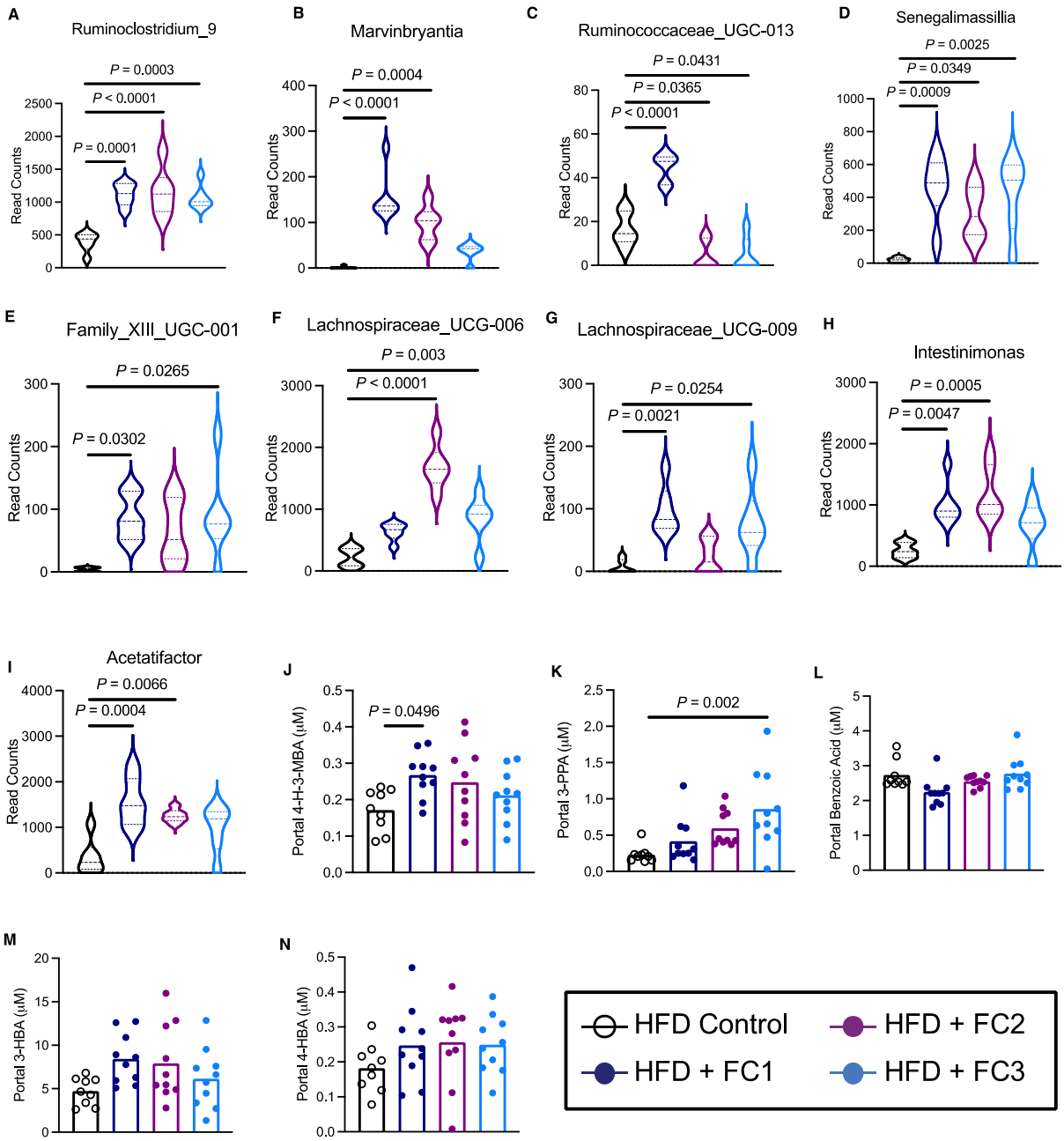

Fig. S3. Flavonoid composite feeding impacts cecal microbiome and portal plasma flavonoid catabolite levels. (**A-I**) Violin plots of representative differentially abundant bacterial genera identified via 16S rRNA sequencing of cecal contents at the time of necropsy, n=6 per group. Ordinary one-way ANOVA with Tukey's multiple

comparisons test used to analyze**.** (**J-N**) Portal plasma concentration of microbial flavonol catabolites measured by LC-MS/MS, one-way ANOVA with Dunnett's multiple comparisons test; n=9-10 per group. Individual points represent individual mice, and bars represent group means.

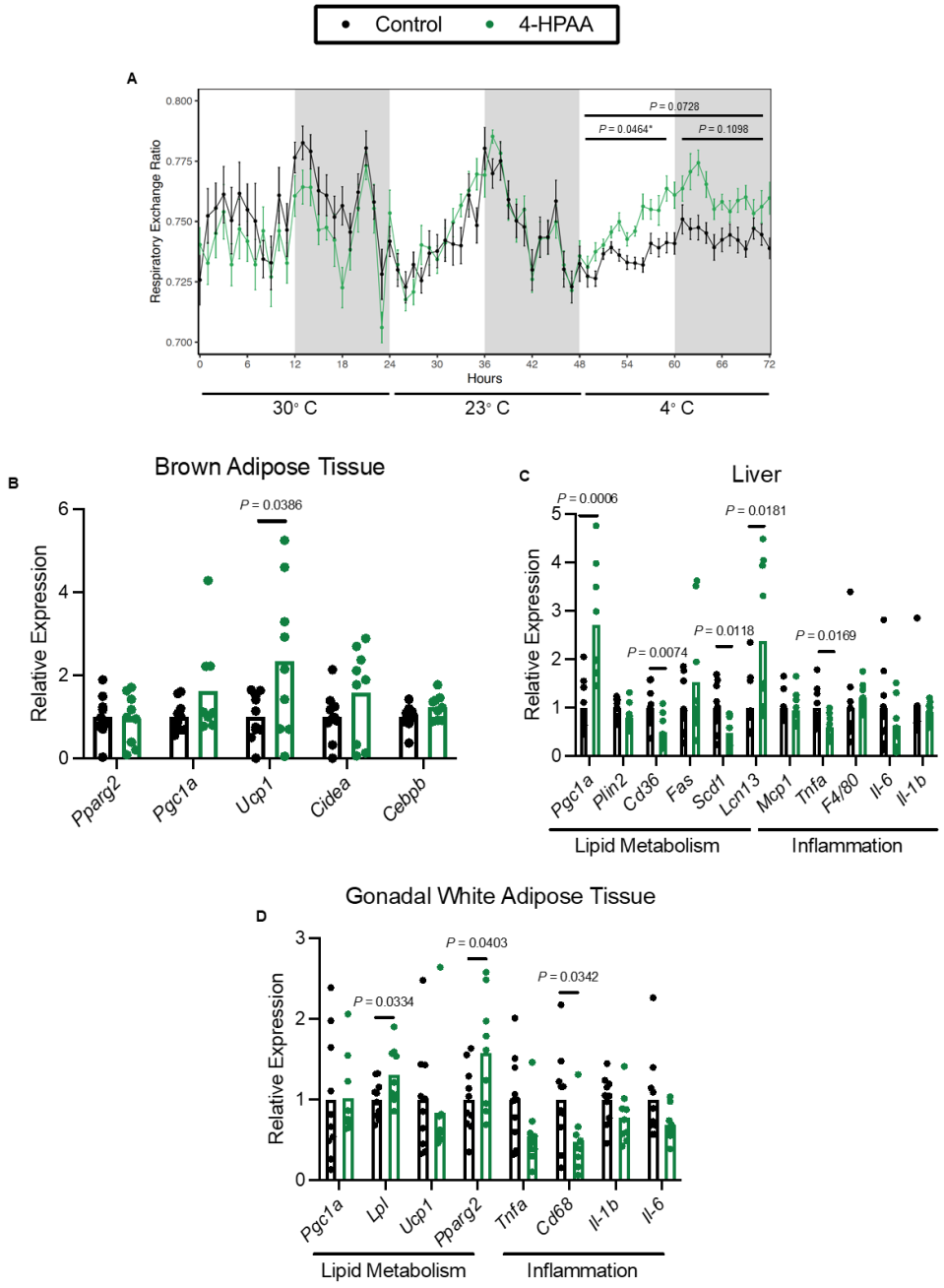

Fig. S4. 4-HPAA treated mice demonstrate improved cold tolerance and transcriptional changes in metabolically active peripheral tissues. (**A**) After twenty-five days of 4-HPAA treatment, global energy substrate utilization was assessed using the Oxymax/CLAMS metabolic cages system, n=6 per group. (**B-D**) RT-qPCR quantification of mRNA transcripts involved in global metabolic programming and

inflammation in brown adipose tissue normalized to the average of *Actb* and *Hprt* (**B**), the liver normalized to *Ppia* (**C**), and gonadal white adipose tissue normalized to *Tbp or Ppia* (**D**), n=9-10 per group. Statistical analysis of Oxymax/CLAMS data was performed using ANOVA in CalR(47). Statistical analysis of RT-qPCR data was performed using unpaired two-tailed Student's t-test. Individual points represent individual mice, and bars represent group means.

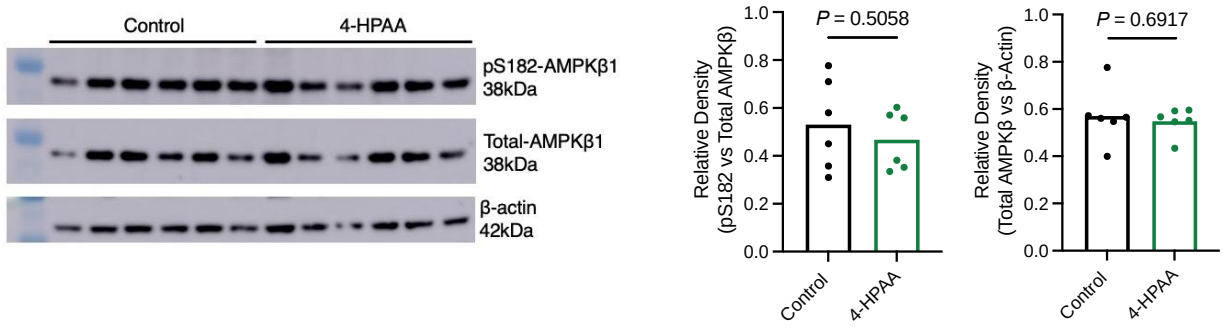

Fig. S5. 4-HPAA does not activate AMPKb in mice. Western blot analysis of pAMPKβ1 (S182), total AMPKβ1, and β-actin with densitometric quantification, n=6 per group. Statistical analysis was performed using an unpaired two-tailed Student's t test. Each dot represents an individual mouse.

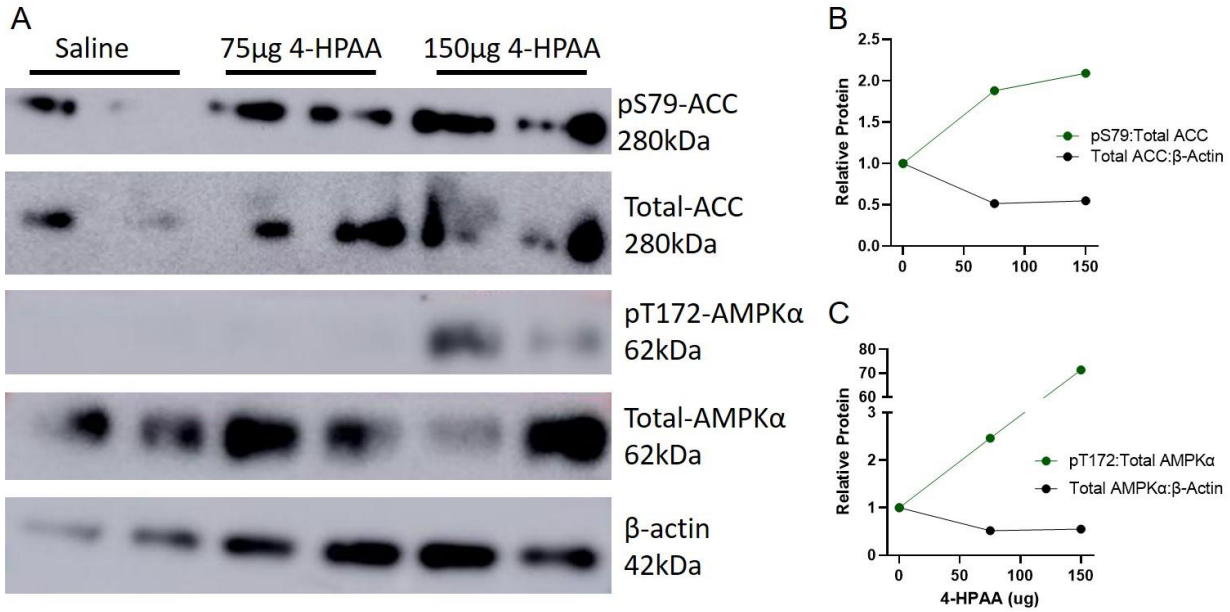

Fig. S6. Direct administration of 4-HPAA to the liver via the portal vein activates AMPK pathway and downstream effectors to reduce de novo hepatic lipogenesis. **(A)** Western blot analysis of pACC (S79), total ACC, pAMPKα (T172), total AMPKα and β-actin. n=2 per group **(B)** Densitometric analysis of pACC (S79) and total ACC from mice injected with either saline control (0 µg), 75, or 150 µg of 4-HPAA. n=2 per group. **(C)** Densitometric analysis of pAMPKα (T172), total AMPKα from mice injected with either saline control (0 µg), 75, or 150 µg of 4-HPAA. n=2 per group.

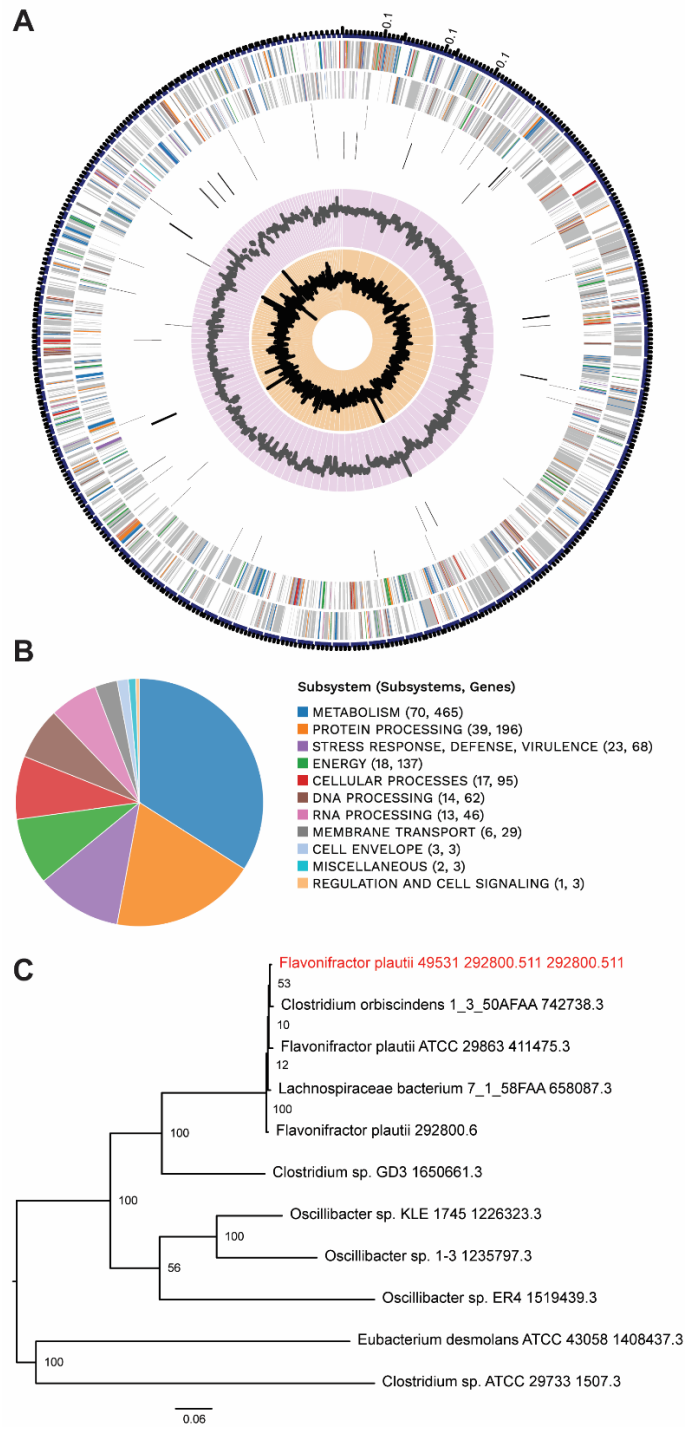

Fig. S7. *Flavonifractor plautii* ATCC 49531 genome composition and phylogeny.

(**A**) A circular graphical display of the distribution of the genome annotations. From outer to inner rings, the contigs, CDS on the forward strand, CDS on the reverse strand,

RNA genes, CDS with homology to known antimicrobial resistance genes, CDS with homology to know virulence factors, GC content and GC skew. The colors of the CDS on the forward and reverse strand indicate the subsystem that these genes belong to as summarized in (**B**). Only the largest 129 contigs are shown. (**C**) Phylogenetic analysis of the *F. plautii* ATCC 49531 genome.

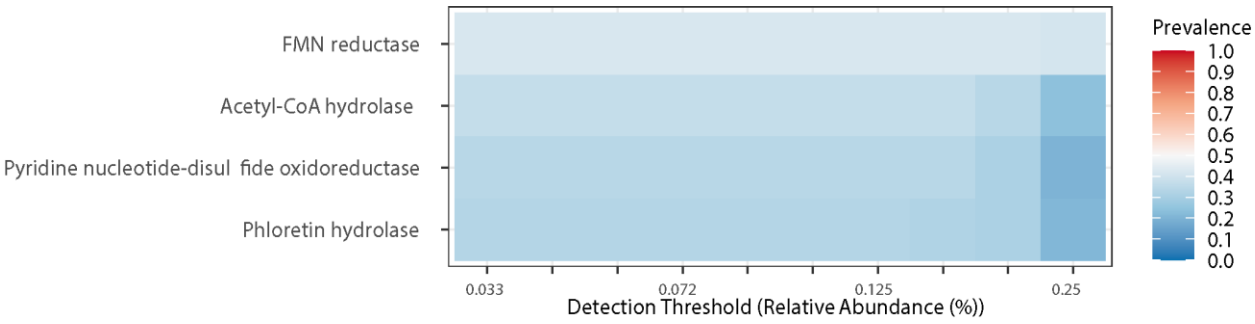

Fig. S8. Shotgun metagenomics data demonstrate the consistent prevalence of *F. plautii* in healthy microbiomes. Relative abundance of *F. plautii* and prevalence of the key marker genes (FMN reductase, Acetyl-CoA hydrolase, Pyridine nucleotide-disulfide oxidoreductase, and Phloretin hydrolase) were measured using Metaphlan2 and whole genome mapping, respectively. Minimum % relative abundance threshold = 0.03349% using the shallowest sequenced sample (11Mbp, and 46,674 reads).

Dataset S1. Metadata for metagenomic sequencing analysis.

Dataset S1.xlsx

Dataset S2. Relative abundance analysis of metagenomic sequencing data.

Dataset S2.xlsx

Dataset S3. Mapping of Poyet *et al.* 2019 data onto the *F. plautii* genome.

Dataset S3.xlsx

Dataset S4. Flavonoid composite information.

Dataset S4.xlsx